Desalination and Water Treatment
www.deswater.com

doi: 10.5004/dwt.2018.22621

118 (2018) 274–280
June

Fluoride removal behavior by aluminum- and lanthanum-doped bioadsorbents

J.J. García-Sánchez[a], M. Solache-Ríos[b,*], S. Ventura-Cruz[c], V. Martínez-Miranda[d], A. Teutli-Sequeira[e]

[a]*Tecnológico de Estudios Superiores de Jocotitlán, Carretera Toluca-Atlacomulco Km 44.8, Ejido de San Juan y San Agustín Jocotitlán, 50700 Jocotitlán, México, email: jjuangs1@gmail.com*
[b]*Instituto Nacional de Investigaciones Nucleares, Carr. México-Toluca S/N (km. 36.5), 52750 Edo de México, México, Tel. +52 5553297200×2271; fax: +52 5553297301; email: marcos.solache@inin.gob.mx*
[c]*Tecnológico de Estudios Superiores de Villa Guerrero, Carretera Federal Toluca Ixtapan de la Sal Km. 64.5, La Finca, 51760 Villa Guerrero, México, email: sagnitev@yahoo.com*
[d]*Centro Interamericano de Recursos del Agua, Facultad de Ingeniería, Universidad Autónoma del Estado de México, Carretera Toluca-Ixtlahuaca, Toluca, Estado de México, México, email: mirandav@uaemex.mx*
[e]*Cátedras CONACYT-Centro Interamericano de Recursos del Agua, Facultad de Ingeniería Universidad Autónoma del Estado de México, km. 14.5, Carretera Toluca-Ixtlahuaca, Toluca, Estado de México, México, email: aleteutli82@yahoo.com.mx*

Received 30 January 2018; Accepted 16 June 2018

ABSTRACT

The use of rose wastes (stem) as a potential alternative and low-cost adsorbent for the removal of fluoride ions was studied. Rose stem (RS) was doped with aluminum or lanthanum ions (RS-Al and RS-La) to increase the fluoride removal efficiency from aqueous solutions. The effects on the structure and physicochemical properties of the RS-doped were also investigated by scanning electron microscopy and energy dispersive spectroscopy and infrared spectroscopy. The best conditions to achieve an efficient adsorption of fluoride ions were evaluated in a batch process. A removal higher than 90% was obtained using a F^- concentration of 5.0 mg/L and pH of 6.5. The sorption equilibrium was reached in 48 h and the kinetic data were treated with the pseudo-second-order model, the results indicated a chemisorption mechanism. The equilibrium of the process was modeled using the Temkin, Freundlich, and Langmuir isotherms, obtaining a best fit with the last one. Finally the thermodynamic parameters of the adsorption processes were determined and the results indicated that the adsorption processes were endothermic and nonspontaneous.

Keywords: Fluoride; Bioadsorption; Rose stem; Aluminum; Lanthanum

---

1. Introduction

Fluorine water pollution has become of considerable concern due to the fact that fluorine has been widely used in a variety of industries, for example, in the production of aluminum, steel, phosphate fertilizers, phosphoric acid, glass, ceramic, and brick products. Fluoride can be found in drinking water, and it is considered hazardous if it exceeds 1.5 mg/L [1]. The excessive intake with long-term drinking of water containing high fluoride concentration can result in health issues, such as mottling of teeth, softening of bones, structural damage to ligaments, and various neurologic damages [2].

A variety of treatment processes have been studied for fluoride removal from drinking water [3]. The adsorption process has been proven to be one of the best water treatment technologies and biosorption is highly important in the environment and conventional biotreatment processes. The biosorption has been used to remove organic

---

* Corresponding author.

and inorganic substances from solution by using different organic materials [4].

Agricultural residues are abundant, cheap, and sustainable materials for the production of bioadsorbents. It is well known that the presence of some of the active components in these materials are lignocellulosic, makes them effective adsorbents for a wide range of pollutants and allow them to efficiently capture water pollutants due to their functional groups such as hydroxyl, carboxyl, methoxy, and phenols that participate in the binding to pollutants. The biodegradability, biocompatibility, and physical–mechanical properties of rose stem (RS), resulting from the presence of chemical reactive groups (hydroxyl, acetamido. or amino functions) in polymer chains can favor the fluoride adsorption [5–9].

The rose is regarded as the queen of flowers because of its aesthetic, beauty, and high economic value; it is one of the most popular flowers. The volume of Mexican rose exports in 2014 reached 2,577 tons, which generated a trade surplus of over 6 million USD during the same year. The states with the highest production are located in the central area of the country, State of México contributes with 7.6 million of gross (a gross refers to a group of 144 items, a dozen of dozens), Morelos, with 647,768; Querétaro with 465.7 thousand, and Puebla with 312.4 thousand gross [10]. The fruits, seeds, and stem of the rose species are considerably beneficial for human health since they contain organic and inorganic matters. The fruits are rich in minerals, vitamins, sugars, phenolic compounds, carotenoids, tocopherol, bioflavonoids, tannins, organic acids, fruit acids, amino acids, volatile oils, and pectin [11]. The seeds of rose also contain unsaturated and polyunsaturated fatty acids [12].

This study considers aluminum- or lanthanum-doped RS as adsorbents for the removal of fluoride ions from aqueous solutions. Results concerning the adsorption equilibrium, kinetics, and thermodynamic are presented and discussed. The effect of various parameters on the process such as pH, contact time, and initial concentration of fluoride were studied. The physicochemical characteristics of the adsorption process were determined; the equilibrium of the process was modeled using the Temkin, Freundlich, and Langmuir isotherms models and the kinetics through the equations of the first- and second-order, Elovich, and intraparticle diffusion models.

2. Experimental

2.1. Collection and preparation of the adsorbent

The stems of rose (SR) were obtained from the rose-flowers production wastes in greenhouses from Villa Guerrero, State of México. They were washed and dried at 60°C for 72 h. Subsequently, they were milled and sieved to produce particles between 50 and 100 meshes (0.297 and 0.149 mm).

2.2. Stock solution and modifying solution

Solutions of 5 mg F^-/L of pH 6.5 were prepared from a standard sodium fluoride solution of 100 mg F^-/L (Thermo Fisher Scientific, USA) and deionized water. Aluminum sulfate (99.99% trace metals basis, Sigma-Aldrich, USA), lanthanum chloride heptahydrate (99.9%, Fisher Scientific), and potassium hydroxide (ACS reagent, ≥97.0%, pellets, Sigma-Aldrich) were used to prepare the solutions.

2.3. Doped stem of rose

Aluminum- and lanthanum-doped stem of rose, were prepared by adding a 2 M KOH solution to a 0.1 M solution of lanthanum or aluminum chloride up to a pH of 7.5. The precipitates were washed three times with distilled water to eliminate K^+ and Cl^- ions from the solids. The lanthanum hydroxide or aluminum hydroxide were mixed with the SR in distilled water, the mixtures were shaken for 4 h, and finally, the water was decanted and the samples were dried at 50°C for 5 h, the samples were labeled as SR-Al or SR-La.

2.4. Characterization of adsorbent

Characterization of biosorbent stems of rose was done before and after doped with Al or La by infrared spectroscopy (IR), scanning electron microscopy (SEM), and energy dispersive spectroscopy (EDS) techniques.

2.4.1. Scanning electron microscopy

The materials were mounted directly on the holders and then observed at 10 and 20 kV in a JEOL JSM-5900-LD electron microscope. The microanalysis was done with an EDS (energy X-ray dispersive spectroscopy) system.

2.4.2. Fourier transform infrared spectroscopy

In order to determine the functional groups responsible for fluoride biosorption, IR spectroscopy was used, about 0.1 g biomass was mixed with KBr for Fourier transform infrared (FTIR) spectra analysis with a resolution of 2 cm^{-1}.

2.5. Determination of surface acidity and basicity

Both the surface acidity and basicity of undoped and doped stems were determined by a titration methods reported by Moreno-Castilla et al. [13] and Güzel [14]. The SR-doped sample were washed several times with distilled water and then dried at 100°C for 24 h prior to titration.

2.5.1. Surface acidity

1 g of RS-doped was prepared as described earlier and put into contact with 50 mL of a 0.1 N NaOH solution. The samples were shaken at 30°C for 5 d using an automatic shaker. The mixture was filtered and then the remaining solution was back-titrated with a 0.1 N HCl solution. The concentrations of acidic and basic groups on the surface were determined and expressed as equivalents per gram (eq/g).

2.5.2. Surface basicity

The total surface basicity of the SR-doped was quantified by mixing 1 g of the adsorbent sample with 50 mL of a 0.1 N HCl standard solution. The mixture was shaken for 5 d at 30°C. An aliquot (10 mL) of the supernatant was filtered and back-titrated with a 0.1 N solution of NaOH solution.

2.6. Fluoride measurements

The fluoride concentrations in the remaining solutions were measured with a specific ion electrode (ISE301F) by using a total ionic strength adjustment buffer solution (TISAB II with CDTA (trans-1.2-diamino cyclohexane tetra acetic acid, monohydrate) to eliminate the interference of complexing ions.

2.7. Sorption studies

Sorption studies were conducted in batch. Various parameters (pH, shaking time, adsorbate concentration, and temperature) on the adsorption process were considered. For the sorption kinetics, the shaking times were 5, 15, 30, 60 min and 3, 5, 7, 24, 48, 72 h and 10 mL of a fluoride solution (5 mg/L) were used. Later, the samples were centrifuged, decanted, and washed. The test of isotherm was realized with 100 mg samples of doped stem in contact with 10 mL of different concentrations of fluoride ions (2.5, 5, 10, 15, 20, 25, 30, 35, 40, and 45 mg/L). The mixtures were shaken at 45 rpm for 24 h. The samples were centrifuged, decanted and fluoride ions were analyzed, each experiment was done in duplicate. All experiments were carried out at 30°C except for the temperature dependence study where the temperatures were 15°C, 30°C, 45°C, and 60°C (initial fluoride concentration was 5 mg/L). The effect of pH on the fluoride ion uptake by doped stems of rose was determined by using an aqueous fluoride solution of 5 mg/L. pH values of fluoride solutions aliquots of 10 mL were adjusted from 2 to 12 using 0.1 M HCl or 0.1 M NaOH and then 100 mg of adsorbent materials were added.

The amount of metal adsorbed per unit mass was calculated as follows:

$$q_e = \frac{\left(C_i - C_e\right)V}{m} \tag{1}$$

where C_i and C_e are the initial and equilibrium concentration (mg/L), *m* is the mass of the adsorbent (g), and *V* is the volume of the solution (mL).

Percent fluoride ion removal (%) was calculated using the following equation:

$$\% = \frac{\left(C_i - C_e\right)}{C_i} \tag{2}$$

In order to explain the mechanism of the process of biosorption: Temkin, Langmuir, and Freundlich isotherm models, pseudo-first-order and pseudo-second-order rate kinetics, and intraparticle diffusion models were applied to experimental data.

3. Results and discussion

3.1. Bioadsorbent characterization

3.1.1. Scanning electron microscope

The chemical composition expressed as the weight percent of the element of the undoped and doped stems of rose are shown in Table 1. The most abundant elements were carbon and oxygen, followed by lanthanum, potassium, chlorine, and aluminum. The presence of potassium and chlorine in SR-doped could be attributed to the modification process. Fig. 1 shows the morphology of the stem of rose, which forms disperse aggregates which correspond to parenchymal tissue, xylem, and fibers (a). In Figs. 1(b) and (c), the presence of possibly aluminum and lanthanum compounds as white particles are shown.

3.1.2. Infrared spectroscopy

Infrared spectra of undoped and doped stem of rose were obtained (Fig. 2). The main functional groups involved in biosorption process and present on the materials were identified. The spectra of SR, SR-Al, and SR-La showed characteristic bands for stem lignin at 1,500 cm^{-1} [15]. The three spectra showed a wide band at 3,330 cm^{-1} assigned to stretching and bending vibrations of OH group. Bands at 2,916 and 2,850 cm^{-1} stretching vibrations were attributed to functional group =CH–, derived formally from methyl group (–CH_3) and methylene group (=CH_2). For SR-Al, these bands appear with a lower intensity than the other materials due to the interaction between the functional group and the Al ion. The spectra of doped SR show bands at 2,341, 2,360, 2,164, 2,026, and 1,975 cm^{-1} which appear with a higher intensity in comparison with the spectrum of the undoped material, this may be assigned to the interaction of functional group phosphine (P–H) and silane (Si–H) with Al or La ions. There is a decrease of the peak at 1,735 cm^{-1} and band displacement of the SR from 1,601 to 1,625 cm^{-1}, due to the interaction of amine (–NH_2) and carboxyl (–COOH) functional groups with Al and La ions. The peak at 1,735 cm^{-1} is attributed to the C=O stretching vibration of the hemicellulose and at 900 cm^{-1} attributed to cellulose.

The FTIR spectra of the SR-doped with La and Al ions, before and after adsorption of fluoride shows the band at 1,242 cm^{-1} shifted to 1,235 and 1,230 cm^{-1}, respectively. This result implies the possibility of interaction between fluoride ion and silane (Si–CH_3), this may suggest that biosorption could take place through an ion exchange process [16].

3.2. Determination of the active sites

The results on the surface acidity of undoped and doped samples of SR waste treated with 0.1 M NaOH follows the

Table 1
Elemental composition of the undoped and doped stems of rose

Element	RS (%)	RS-Al (%)	RS-La (%)
C	54.0 ± 1.0	46.6 ± 0.7	44.2 ± 1.6
O	42.6 ± 1.3	34.4 ± 0.8	29.3 ± 1.5
Al	0.5 ± 0.6	12.6 ± 0.6	0.6 ± 0.3
K	1.6 ± 0.1	2.7 ± 0.6	1.9 ± 0.3
Ca	0.7 ± 01	–	0.2 ± 0.0
Fe	0.4 ± 0.1	–	–
P	0.2 ± 0.0	–	–
Cl	–	3.7 ± 0.4	4.8 ± 1.1
La	–	–	19.0 ± 2.2

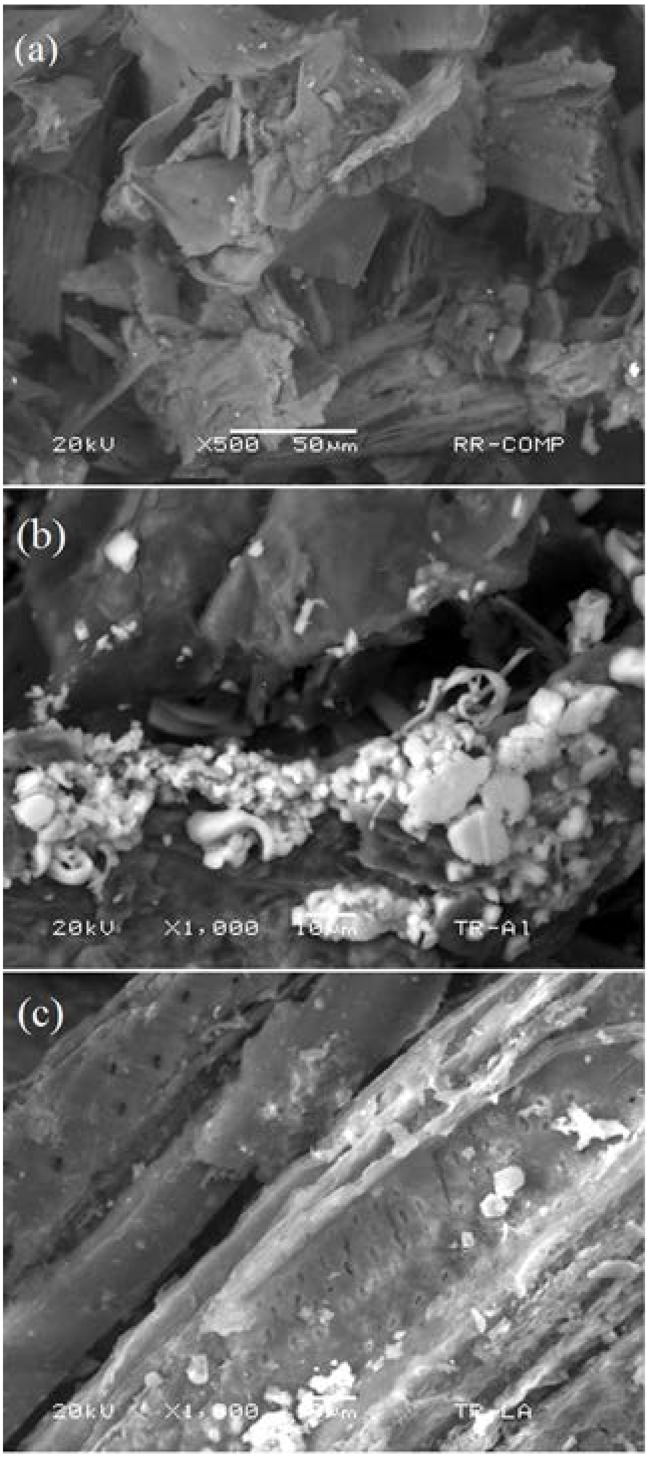

Fig. 1. SEM images of (a) undoped stems of rose, (b) stems of rose doped with aluminum, and (c) stems of rose doped with lanthanum.

order, RS-La (2.4 eq/g) > RS (2.2 eq/g) ≈ RS-Al (2.1 eq/g). The results of surface acidity indicate that RS-La has the highest affinity for the adsorption of acidic components in aqueous solution, while RS-Al exhibited the lowest affinity for acidic species.

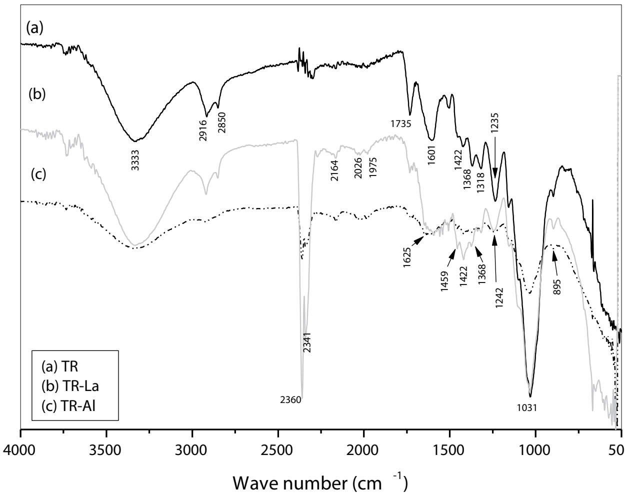

Fig. 2. FTIR spectra of stem of rose before and after doped with La or Al.

The adsorption capacity for basic species in aqueous solution of the SR waste was in the order: SR-La (2.7 eq/g) > SR (2.5 eq/g) > SR-Al (1.7 eq/g). The surface basicity experiment verifies the affinity of the SR for basic species in aqueous solution. The results indicate that SR-La has the highest affinity for basic species in aqueous solution.

The differences between values of the acidic and basic groups suggest that the majority of functional groups on the adsorbent surface are basic; these basic sites favor the surface precipitation of fluoride ions. The number of basic groups is proportional to the adsorption of anions. However the adsorption not only depends on this parameter, it also depends on the affinity of fluoride for the metal present in the adsorbent.

3.3. Adsorption kinetics

The fluoride ions biosorption kinetics of SR-Al and SR-La are shown in Fig. 3. The removal of F^- was found to be 91.2% and 89.6% respectively, at 30°C and pH 6.5. The adsorption was rapid at the beginning of the process and equilibrium was reached in about 24 h. Both materials, SR-Al and SR-La, exhibited analogous behavior during fluoride removal, with similar efficiencies. The kinetic data analysis for fluoride sorption onto different materials has been treated with different models: pseudo-first-order (Eq. (3)), pseudo-second-order (Eq. (4)), and intraparticle diffusion (Eq. (5)) models by a linear regression analysis (Table 3). The equations of these models are as follows [17,18]:

$$\log\left(q_e - q_t\right) = \log\left(q_e\right) - \left(K_1 / 2.303\right)t \tag{3}$$

$$t / q_t = 1 / K_2 q_e^2 + \left(1 / q_e\right)t \tag{4}$$

$$q_t = K_i t^{0.5} + C \tag{5}$$

where q_e and q_t are the sorption capacities at equilibrium and at time t, respectively (mg/g). K_1 is the rate constant of pseudo-first-order sorption (h^{-1}), K_2 is a constant of

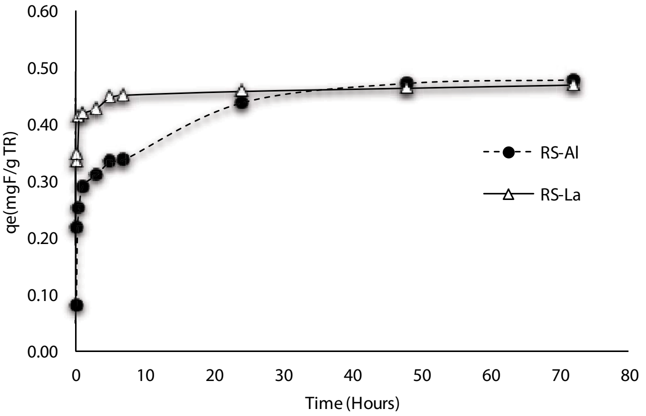

Fig. 3. Contact time versus sorption capacity of fluoride (0.1 g of sorbent in 10 mL of fluoride solution).

pseudo-second-order (g/mg h), K_i is the intraparticle diffusion rate constant (mg/g h), and C is the intercept (mg/g) of the plot, which reflects the boundary layer effect. The larger the intercept, the greater is the contribution of the surface sorption in the rate controlling step. If the plot of q_t versus $t^{0.5}$ is linear and passes through the origin, then intraparticle diffusion is the sole rate-limiting step [19].

The removal of fluoride ions from aqueous solution involves solute transfer, which is usually characterized by either external mass transfer (boundary layer diffusion) or intraparticle diffusion or both. In order to gain insight into the mechanisms and rate controlling steps affecting the kinetics of adsorption, the kinetic experimental results were fitted to the models.

The experimental data could not be fitted to the pseudo-first-order and intraparticle diffusion kinetic models because the calculated sorption capacities at equilibrium were different from the experimental values and the R^2 values were low. The plot of q_t versus $t^{0.5}$ (intraparticle diffusion model) is not linear and it does not pass through the origin, this indicates that the intraparticle diffusion was not the rate-controlling step. This behavior also confirms that adsorption of fluoride ions on the adsorbent was a process which involves adsorption on the external surface [20].

The experimental data were adjusted to the pseudo-second-order model, the adsorption capacities were 0.48 and 0.47 mg/g and the values of K_2 were 1.7 and 10.7 g mg/h with R^2 of 0.9985 and 0.9999 for both SR-Al and SR-La, respectively. The model is based on the assumption that the rate-limiting step may be chemisorption involving valence forces through sharing or exchange of electrons between adsorbent and adsorbate. It is important to note that similar experiments were performed with SR and the adsorption was only 27% in comparison with the adsorption shown by SR-Al and SR-La.

3.4. Adsorption equilibrium

The adsorption yields were around 99% from initial fluoride concentrations ranging between 1 and 6 mg/L and then decreased as the initial fluoride concentrations increased from 9 to 30 mg/L.

Equilibrium studies were carried out in order to determine the optimum conditions for maximum fluoride removal by the SR-doped. The analysis of the isotherms data was performed by fitting them to different isotherm models; this is an important step to find out the suitable model that can be used for designing purposes. In this work, the isotherms obtained (Fig. 4) were fitted to the Langmuir [21] (Eq. (6)), Freundlich [22] (Eq. (7)), and Temkin [23] (Eq. (8)) models by linear regression analysis, in order to describe the relationship between the amount of fluoride ion adsorbed (q_e), and its equilibrium concentration (C_e), by SR-Al and SR-La. The linear equations of the isotherms of these models are as follows:

$$\frac{C_e}{q_e} = \frac{1}{Q^0 b} + \frac{1}{Q^0} C_e \tag{6}$$

$$\log(q_e) = \log K_F + \frac{1}{n} \log(C_e) \tag{7}$$

$$q_e = B \ln K_T + B \ln C_e \tag{8}$$

where C_e is the fluoride concentration in solution at equilibrium (mg/L), q_e is the amount of adsorbed dye per unit mass of adsorbent (mg/g). Q^0 and b are Langmuir isotherm constants related to the theoretical maximum adsorption capacity (mg/g) and the energy of adsorption (L/g), respectively. K_F is the Freundlich constant representing the adsorption capacity (L/g), and n is the Freundlich exponent that indicates the adsorption intensity (dimensionless). K_T and B are the Temkin isotherm constants, where K_T represents the equilibrium binding constant (L/g) and B is the heat of adsorption and $B = RT/b$.

The constants of linearized forms of Langmuir, Freundlich, and Temkin isotherms were calculated from the intercept and slope of the plot C_e/q_e versus C_e, log q_e versus log C_e, and q_e versus ln C_e, respectively. The equilibrium experimental results of fluoride ions could not be fitted to the linear forms of Freundlich and Temkin models because the R^2 values were low (<0.9256). The experimental data were found to fit the Langmuir isotherm. The linearity of the plots C_e/q_e versus C_e showed the applicability of the Langmuir isotherm to the experimental data. The basic assumption of Langmuir adsorption isotherm is based on monolayer coverage of the adsorbate on the surface of adsorbent. Q^0 and b were determined from the slopes and intercepts of the respective plots (Table 2). In order to find out the feasibility of the isotherm,

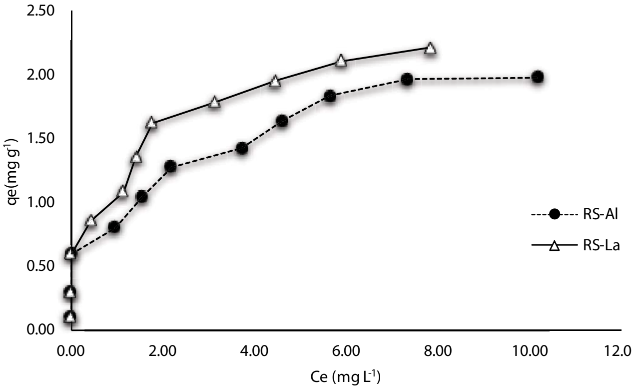

Fig. 4. Sorption isotherm of fluoride ions by SR-Al or SR-La.

Table 2
Adsorption isotherms parameters of fluoride ions sorption by RS-doped with Al or La

Adsorbent materials	Langmuir			
	b (L/g)	Q^0 (mg/g)	R^2	R_L
RS-Al	1.27	2.06	0.9639	0.1021
RS-La	1.91	2.26	0.9757	0.0741

the essential characteristics of the Langmuir isotherm can be expressed in terms of the dimensionless constant separation factor or equilibrium parameter [21].

$$R_L = \frac{1}{1 + bC_0} \tag{9}$$

where b is the Langmuir isotherm constant and C_o is the initial concentration of fluoride (mg/L).

The adsorption capacities calculated from Langmuir isotherm constants were found to be 2.06 and 2.26 mg/g for SR-Al and SR-La, respectively. The maximum monolayer capacity of the adsorbent Q^0, indicated that SR-La possessed a higher adsorption capacity than SR-Al. The lanthanum hydroxide has a high affinity for fluoride ions and it has been reported there is not any significant influence of competing anions on its defluoridation capacity [24]. Also, R_L values were between 0 and 1, indicating that the adsorption of fluoride ions on SR-doped was favorable.

3.5. Effect of pH on the sorption of fluoride ions by the bioadsorbents

The effect of pH on the sorption is an important parameter because the removal of the fluoride ions from the aqueous solution depends on the solution pH, as it alters the surface charge on the adsorbents [25].

The decrease of fluoride uptake by SR-La (Fig. 5) in alkaline pH could be primarily influenced by the competition for active sites by fluoride ions and the excessive amount of hydroxyl ions [26]. The adsorption process can be explained on the basis that the adsorbents contain aluminum or lanthanum hydroxides and these hydroxides have the tendency to form complexes with the fluoride ions. Similar results can be found in studies reported by García-Sánchez et al. [26,27], using modified corrosion products with La and modified natural magnetite with Al and La ions. Although the adsorption of SR-Al is slightly higher than SR-La at pH ≤ 10, it is important to note that at pH 12, SR-Al is more efficient than SR-La, the stability of the complexes formed should be responsible for this behavior.

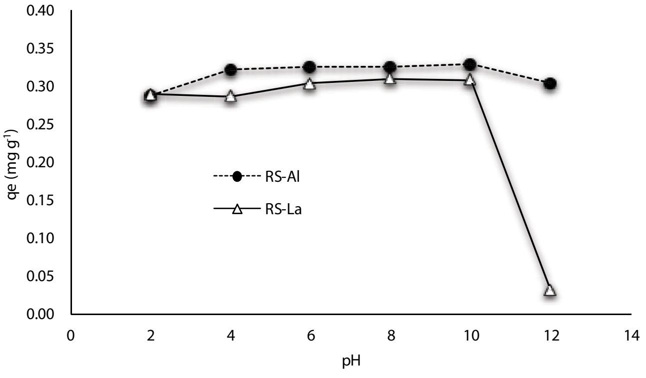

Fig. 5. Effect of pH on the removal of fluoride ions by RS-Al or RS-La.

3.6. Effect of temperature on bioadsorption of fluoride ions

The effect of temperature on the sorption of fluoride ions on SR doped with La or Al was also investigated using the optimized conditions. It was observed that the sorption of fluoride increases with the increase of temperature (Table 3). The increase in the removal of the fluoride ions with an increase of temperature may be due to the mobility of the ionic species present in the bulk solution at higher temperatures. The collision frequency between the adsorbent and adsorbate increased and hence the adsorption on the surface of the adsorbent increased [28].

Thermodynamic parameters are calculated from the variation of the thermodynamic equilibrium constants (K_c) at different temperatures (15°C, 30°C, 45°C, and 60°C) by using the following equations (Table 4):

$$K_c = \frac{q_e}{C_e} \tag{10}$$

$$\ln K_c = -\frac{\Delta H^0}{R \times T} + \frac{\Delta S^0}{R} \tag{11}$$

$$\Delta G^0 = \Delta H^0 - T \times \Delta S^0 \tag{12}$$

Table 3
Temperature effect on the percentage of fluoride ions sorbed on SR-doped with Al or La at equilibrium

Temperature (°C)		15	30	45	60
Adsorption (%)	SR-Al	81.9	85.2	86.9	90.1
	SR-La	86.3	87.3	88.8	90.6

Table 4
Thermodynamic parameters for sorption of fluoride on SR-doped with Al or La as a function of temperature

T (°C)	$\Delta G°$ (kJ/mol)	$\Delta H°$ (kJ/mol)	$\Delta S°$ (J/mol K)
SR-Al			
15	1.94	11.83	34.31
30	1.43		
45	0.91		
60	0.40		
SR-La			
15	1.18	7.38	21.53
30	0.85		
45	0.53		
60	0.21		

where $\Delta H°$, $\Delta S°$, $\Delta G°$, and T are the standard enthalpy, standard entropy, Gibbs free energy, and temperature in kelvin, respectively, and R is the gas constant in kJ/mol/K.

The enthalpy and entropy were calculated from the slope of straight line plot of log K_c versus $1/T$, derived from the application of the Van't Hoff [29], whereas $\Delta G°$ was evaluated using Eq. (12).

The positive values of $\Delta G°$ indicate, the adsorption process is nonspontaneous. The values of $\Delta S°$ were found to be 34.31 and 21.53 J/K/mol for SR-Al and SR-La, respectively, and positive values indicate that the degree of freedom of ions increased by sorption and also is an indication of the stability of surface sorption. The values of $\Delta H°$ are positive and it confirms the endothermic character of the reaction [30].

4. Conclusions

The experimental results show that doped SR was effective for the removal of defluoride ions from aqueous solution. The kinetic and isotherm results could be adjusted to the pseudo-second-order model and to the Langmuir model, respectively, which indicate that the sorption mechanism is chemisorptions on a homogeneous material. The maximum adsorption capacities from Langmuir isotherm were found to be 2.06 and 2.26 mg/g for SR-Al and SR-La, respectively. According to the effect of the temperature on bioadsorption of fluoride ions, the adsorption process is nonspontaneous and endothermic. The agro-industrial residues used in this work are locally available and abundant; the resulting sorbent is economically viable for removal of fluoride ions from aqueous solutions. This study also offers a solution to the reduction of agro-industrial solid waste, potentially limiting its adverse environmental impacts.

Acknowledgment

We acknowledge financial support from PRODEP, project 197241.

References

[1] World Health Organization (WHO), Guidelines for Drinking-Water Quality, 4th ed., 2012, pp. 370–373. ISBN 978 92 4 154815 1.

[2] Y. Zhang, L. Yang, D. Wang, T. Zhang, Resource utilization of water treatment residual sludge (WTRS): effective defluoridation from aqueous solution, Desal. Wat. Treat., 55 (2015) 448–462.

[3] J. Kyung-Won, H. Min-Jin, J. Tae-Un, C. Dao Minh, K. Kipal, A. Kyu-Hong, Entrapment of powdered drinking water treatment residues in calcium-alginate beads for fluoride removal from actual industrial wastewater, J. Ind. Eng. Chem., 39 (2016) 101–111.

[4] M. Fomina, G.M. Gadd, Biosorption: current perspectives on concept, definition and application, Bioresour. Technol., 160 (2014) 3–14.

[5] B.H. Hameed, R.R. Krishni, S.A. Sata, A novel agricultural waste adsorbent for the removal of cationic dye from aqueous solutions, J. Hazard. Mater., 162 (2009) 305–311.

[6] S.J. Allen, B. Koumanova, Decolourisation of water/wastewater using adsorption, J. Univ. Chem. Technol. Metall., 40 (2005) 175–192.

[7] M. Bansal, U. Garg, D. Singh, V.K. Garg, Removal of Cr (VI) from aqueous solutions using pre-consumer processing agricultural waste: a case study of rice husk, J. Hazard. Mater., 162 (2009) 312–320.

[8] M. Habuda-Stanić, M.E. Ravančić, A. Flanagan, A review on adsorption of fluoride from aqueous solution, Materials, 7 (2014) 6317–6366.

[9] P.K. Raul, R.R. Devi, I.M. Umlong, S. Banerjee, L. Singh, M. Purkait, Removal of fluoride from water using iron oxide-hydroxide nanoparticles, J. Nanosci. Nanotechnol., 12 (2012) 3922–3930.

[10] (SIAP), Servicio de Información Agroalimentaria y Pesquera, (Food, Agriculture and Fishing Information Service) (2015), Food & Agriculture Atlas, 1st ed., 2015.

[11] S. Ercisli, Chemical composition of fruits in some rose (*Rosa* spp.) species, Food Chem., 104 (2007) 1379–1384.

[12] K. Szentmihályi, P. Vinkler, B. Lakatos, V. Illes, M. Then, Rose hip (*Rosa canina* L.) oil obtained from waste hip seeds by different extraction methods, Bioresour. Technol., 82 (2002) 195–201.

[13] C. Moreno-Castilla, F. Carrasco-Marin, E. Utrera-Hidalgo, J. Rivera-Utrilla, Effect of their pore texture and surface basicity, Langmuir, 9 (1993) 1378–1383.

[14] F. Güzel, The effect of surface acidity upon the adsorption capacities of activated carbons, Sep. Sci. Technol., 31 (1996) 283–290.

[15] W. Jonglertjunya, T. Juntang, N. Pakkang, N. Srimant, C. Sakdaronnarong, Properties of lignin extracted from sugarcane bagasse and its efficacy in maintaining post-harvest quality of limes during storage, Food Sci. Technol., 57 (2014) 116–125.

[16] E.M. Schneider, M.Z. Eltner, V. Zlateski, R.N. Grass, W.J. Stark, Click and release: fluoride cleavable linker for mild bioorthogonal separation, Chem. Commun., 52 (2016) 938–941.

[17] W.J. Weber, J.C. Morris, Kinetics of adsorption on carbon solution, J. Sanit. Eng. Div. ASCE, 89 (1993) 31–59.

[18] Y.S. Ho, G. McKay, Application of kinetics models to the sorption of copper (II) on to peat, Adsorpt. Sci. Technol., 20 (2002) 797–815.

[19] Y.S. Ho, Removal of copper ions from aqueous solution by tree fem, Water Res., 37 (2003) 2323–2330.

[20] K.G. Bhattacharyya, A. Sharma, Kinetics and thermodynamics of methylene blue adsorption on Neem (*Azadirachta indica*) leaf powder, Dyes Pigments, 65 (2005) 51–59.

[21] G. Bitton, Formula Handbook for Environmental Engineers and Scientists, Wiley, NY, 1998.

[22] Y.S. Ho, J.C.Y. Ng, G. McKay, Removal of lead(ii) from effluents by sorption on peat using second-order kinetics, Sep. Sci. Technol., 36 (2001) 241–261.

[23] A. Kausar, H.N. Bhatti, G. MacKinnon, Equilibrium, kinetic and thermodynamic studies on the removal of U (VI) by low cost agricultural waste, Colloids Surf., B, 111 (2013) 124–133.

[24] N. Choon-Ki, P. Hyun-Ju, Defluoridation from aqueous solution by lanthanum hydroxide, J. Hazard. Mater., 183 (2010) 512–520.

[25] S. Meenakshi, A. Pius, G. Karthikeyan, B.V. Appa Rao, The pH dependent of efficiency of activated alumina in defluoridation of water, Indian J. Environ. Prot., 11 (1991) 511–513.

[26] J.J. García-Sánchez, M. Solache-Ríos, J.M. Martínez-Gutiérrez, N.V. Arteaga-Larios, M.C. Ojeda-Escamilla, I. Rodríguez-Torres, Modified natural magnetite with Al and La ions for the adsorption of fluoride ions from aqueous solutions, J. Fluorine Chem., 186 (2016) 115–124.

[27] J.J. García-Sánchez, M. Solache-Ríos, V. Martínez-Miranda, Behavior of fluoride ions in the presence of lanthanum and magnesium modified corrosion products, Sep. Sci. Technol., 50 (2015) 1461–1468.

[28] E. Oguz, Adsorption of fluoride on gas concrete materials, J. Hazard. Mater., 117 (2005) 227–233.

[29] G. Karthikeyan, S. Siva Ilango, Fluoride sorption using *Morringa indica*-based activated carbon, Iran J. Environ. Health Sci. Eng., 4 (2007) 21–28.

[30] Z. Bouberka, S. Kaoha, M. Kamecha, S. Elmaleh, Z. Derriche, Sorption study of an acid dye from aqueous solutions using modified clays, J. Hazard. Mater., 119 (2005) 117–124.